Available online at www.sciencedirect.com
SCIENCE DIRECT®
Catalysis Today 89 (2004) 369–374
CATALYSIS TODAY
www.elsevier.com/locate/cattod

Effect of oxygen on the Mn–Co ferromagnetic coupling

Štěpán Pick [a,*], Claude Demangeat [b]

[a] *J. Heyrovský Institute of Physical Chemistry, Academy of Sciences of the Czech Republic, Dolejškova 3, CZ-182 23 Prague 8, Czech Republic*
[b] *Institut de Physique et de Chimie des Matériaux de Strasbourg, 23 Rue du Loess, F-67037 Strasbourg, France*

Abstract

The paper describes the study of the effect of oxidation on the magnetic coupling between Mn and Co atoms in ultrathin Mn films deposited on fcc Co(0 0 1). The magnetic map has been investigated through tight-binding linear-muffin-tin scheme within generalized gradient approximation of the density functional. The calculations indicate that oxygen tends to destabilize the ferromagnetic Mn–Co coupling in favour of an antiferromagnetic coupling found by experiment when oxygen is added. Nevertheless, the (1×1) structures observed do not seem to be the most stable ones. We speculate that a disordered oxidized Mn-rich MnCo surface alloy might explain the experimental findings.

Keywords: Density-functional calculations; Ultrathin magnetic films; Oxygen chemisorption; Cobalt; Manganese; Antiferromagnetic coupling; Ferromagnetic coupling

1. Introduction

Since the X-ray magnetic circular dichroism (XMCD) results of O'Brien and Tonner [1] considerable attention has been attracted by Mn adsorption on fcc Co(0 0 1) films. These authors concluded that the coupling between Mn deposited in ultrathin overlayer and Co was of ferromagnetic (F) type, but rather than MnCo alloying a nonideal Mn overlayer(s) was suggested to grow at the Mn–Co interface. Noguera et al. [2], using a tight-binding Hamiltonian, were unable to obtain the F coupling for a perfect Mn monolayer epitaxially grown on fcc Co(0 0 1). Later on, Elmouhssine [3] performed a tight-binding linear-muffin-tin-orbital (TB-LMTO) in the atomic sphere approximation within local density approximation (LDA). His result confirms the in-plane antiferromagnetic (AF) $c(2 \times 2)$ configuration as the ground state and is at odd with the XMCD results of O'Brien and Tonner [1]. He obtained also (besides others) metastable in-plane ferromagnetic Mn overlayer with a difference of energy as high as 20 mRy per Mn atom. From this calculation, it was concluded that a perfect Mn monolayer grown on Co(0 0 1) is only a very simplified theoretical approximation so that Meza-Aguilar [4] extended the calculations to various ordered MnCo alloys at the Mn–Co interfaces. These calculations were directly related to very careful low-energy electron diffraction (LEED), magneto-optic Kerr effect (MOKE) and XMCD measurements by O'Brien and Tonner [5] and Choi et al. [6] displaying some kind of ordered MnCo alloy at the interface. From their LEED experiments, Choi et al. [6] deduced formation of a $c(2 \times 2)$ chemically ordered MnCo magnetic surface alloy, where Mn is predominantly aligned ferromagnetically with respect to the Co(0 0 1) substrate. This was indeed the first report about the existence of a MnCo magnetic surface alloy already postulated by O'Brien and Tonner [5]. Although ferromagnetic coupling was observed just after the deposition of Mn on Co(0 0 1), it was found to be reversed as oxidation of the Mn film proceeded [5].

The recent detailed experimental study of Yonamoto et al. [7] is consistent with the measurements of Ref. [5]. However, the authors arrived to the conclusion that "These discrepancies between experiments can now be explained by the effect of oxidation". According to our opinion the situation is more complicated. Meza-Aguilar et al. [8] have performed, following the LEED results of Choi et al. [6] a TB-LMTO-LDA calculation of an ordered MnCo alloy (1 and 2 MLs thick) on Co(0 0 1) in order to check whether or not these configurations are more stable as compared to the perfect Mn monolayer on Co(0 0 1). It has been shown that these alloy configurations are indeed more stable. Moreover, they find that an inverted Mn–Co

* Corresponding author. Tel.: +420-266053496; fax: +420-28582307.
E-mail address: pick@jh-inst.cas.cz (Š. Pick).

0920-5861/$ – see front matter © 2003 Elsevier B.V. All rights reserved.
doi:10.1016/j.cattod.2003.12.010

configuration, i.e. Co/Mn/Co(0 0 1) is more stable as compared to $Mn_{0.5}Co_{0.5}/Mn_{0.5}Co_{0.5}$/Co(0 0 1). This has not been observed experimentally [6], probably because of a kinetic barrier. A similar kinetically hindered capped configuration was anticipated [10] also for Mn–Pd films. An annealing process may overcome it and we expect to see very different magnetic behaviour in that case. Following the LEED results of Choi et al. [6], Meza-Aguilar et al. have, for the specific case of $Mn_{0.5}Co_{0.5}$/Co(0 0 1) shown that: (i) this ordered surface alloy is more stable than the perfect Mn monolayer on Co(0 0 1); (ii) F coupling between Mn and Co has been obtained but this configuration is marginally unstable as compared to the solution with AF coupling. It is interesting to mention that a combined experimental and theoretical (LDA) study [9] of MnCo alloys arrives at Mn–Co F coupling for fcc structures and AF coupling for bcc lattices (the labelling "fcc" and "bcc" is apparently interchanged in Tables 2 and 3 of Ref. [9]).

Mn being the most complex of all metallic elements, LDA may not be the right approximation to describe it. It has been shown by Blügel [11] that the formation of the Mn–Cu surface alloy on Cu(0 0 1) changes sign when going from LDA to the generalized gradient approximation (GGA). Also, Hobbs and Hafner [12] have used gradient corrections to determine the crystalline and magnetic structures of all known polymorphs of Mn. For all these reasons Meza-Aguilar and coworkers [13] have determined the stability and the magnetic map of $Mn_{0.5}Co_{0.5}$/Co(0 0 1) by using two types of gradient corrections [14–16]. Both approaches lead to a ferromagnetic coupling between Mn and Co but only the Perdew–Wang functional displays a stabilization of the surface ordered alloy [13]. This result is now in agreement with the experimental results [1,5,6]. The aim of this paper is to extend the latter study [13] to oxidized Mn–Co films in order to verify the expected modification of the coupling between Mn and Co atoms. Let us note that studies of Mn deposition at the (0 0 1) face of various transition metals have been performed (see discussion and references in papers [5,10]) but no "universal" picture seems to emerge. Recent review of Mn behaviour in various surface structures can be found in Ref. [17].

Throughout the paper, units common in quantum theory are employed. For the convenience of reader, we give here also their conversion into SI units: $1\,\mathrm{eV} = 1.602 \times 10^{-19}\,\mathrm{J}$, $1\,\mathrm{Ry} = 13.605\,\mathrm{eV} = 2.180 \times 10^{-18}\,\mathrm{J}$, $1\mu_B = 9.273 \times 10^{-24}\,\mathrm{J\,T^{-1}}$.

2. Model

In our electronic structure calculations we utilize the tight-binding linear-muffin-tin-orbital code [18] in the atomic-sphere-approximation (ASA). Because of the recent experience [8,13] with the density-functional calculations performed for Mn–Co films, we choose the Langreth–Mehl–Hu and Perdew–Wang exchange-correlation potentials with gradient corrections [14–16]. The starting point are several systems of those investigated in Ref. [8]. Namely, we consider ferromagnetic (0 0 1) fcc cobalt slabs with: (a) epitaxial Mn overlayer or, (b) epitaxial $c(2 \times 2) = (\sqrt{2} \times \sqrt{2})R45^\circ$ ordered MnCo alloy layer. In case (a) we pay attention to an (1×1) homogeneously magnetized Mn layer that couples: (a1) ferromagnetically, (a2) antiferromagnetically to the Co slab, or leads (a3) to an in-plane antiferromagnetic $c(2 \times 2)$ in the Mn overlayer. In case (b) the Mn atoms in the surface alloy can couple F (b1) or AF (b2) to the cobalt atoms. Similarly, as in Ref. [8] we use the supercell approach with repeated nine-layer metal slabs separated by five layers of empty spheres representing vacuum. All atom positions correspond to the ideal fcc structure. The only difference with Refs. [8,13] is that we take a slightly different nearest-neighbour separation of 2.50 Å [9,19,20]. For the most interesting cases (b1) and (b2), we performed an explicit calculation and found quite analogous results as in Ref. [8], with magnetic moments in surface and subsurface layer a bit lower (see Tables 1 and 2) because of our slightly smaller lattice constant. Numerous studies for oxygen adsorption on transition-metal (0 0 1) surfaces show that the four-fold (hollow) site is an obvious choice. We consider a complete oxygen monolayer, and to

Table 1
Results for $c(2 \times 2)$ MnCo/Co(0 0 1) systems without and with oxygen overlayer

System	O	Mn	Co(S)	Co(S-1)	E
MnCo $c(2 \times 2)$, F		3.53	1.60	1.53	00
MnCo $c(2 \times 2)$, AF		−3.63	0.70	1.25	12
O/MnCo $c(2 \times 2)$, F	−0.10	2.24	1.46	1.59	00
O/MnCo $c(2 \times 2)$, AF	0.15	−3.30	1.40	1.47	01

F (AF) means that Mn couples (anti)ferromagnetically to Co. Magnetic moments in μ_B are shown for oxygen, surface Mn, surface (S) and subsurface (S-1) Co atoms. E (mRy) is the energy per unit cell (two atoms in every layer) and per one of the two slab surfaces (i.e. half of the energy of the slab). The energy of the more stable system is put to zero by definition.

Table 2
Results for Mn/Co(0 0 1) systems without and with oxygen overlayer

System	Exp	O	Mn1	Mn2	Co(S-1)	E
Mn (1×1), F	0		3.36	3.36	1.48	33
Mn (1×1), AF	0		−2.99	−2.99	1.10	62
Mn $c(2 \times 2)$	0		3.05	−3.35	1.09	00
O/Mn (1×1), F	0	−0.21	1.27	1.27	1.53	37
O/Mn (1×1), AF	0	−0.06	−0.29	−0.29	1.17	35
O/Mn $c(2 \times 2)$	0	−0.04	2.76	−2.48	1.47	00
O/Mn (1×1), F	10	−0.34	1.55	1.55	1.63	36
O/Mn (1×1), AF	10	[a]	[a]	[a]	[a]	[a]
O/Mn $c(2 \times 2)$	10	−0.01	2.92	−2.64	1.57	00

The meaning of symbols is the same as in Table 1. For (1×1) systems, Mn1 and Mn2 atoms, respectively, are equivalent.

[a] No stable solution has been found. Exp (%) denotes the interlayer distance expansion between the Mn overlayer and subsurface Co layer, respectively. For all structures the energies are related to (2×2) cells to enable proper comparison.

a lesser detail also half-monolayer coverage. The Mn–O separation is fixed at the value 2.2 Å—a guess based on the separation in the crystal Mn–O [9,19] and consistent also with atomic-radii reasoning with the oxygen radius assessed from typical chemisorption data (cf., e.g. Refs. [21,22]). For oxygen above the $c(2\times2)$ MnCo alloy we use the same value also for the Co–O distance. For oxygen above the Mn overlayer, we consider together with the ideal fcc lattice also expansion of the Mn–Co interplanar distance by 10%. The reason is that the metallic radius of Mn is less reliable quantity and perhaps a value somewhat superior to the Co value is more appropriate [9]. Besides that, oxygen adsorption causes such an expansion is some systems [23]. The oxygen is adsorbed on both slab surfaces. To speed up the extremely poorly converging calculations, only three-layer vacuum is used now (cf. [24]). The high symmetry of the supercell (reflection planes) should lead to considerable mutual cancellation of dipolar electrostatic contributions from oxidized surfaces. The charge in the central vacuum spheres is small (about 0.01*e*). Besides that, calculation is somewhat simplified if, for the $c(2\times2)$ structures, the geometry with the central-slab plane representing a *glide* reflection plane is used: the Co atoms lying in the central slab become equivalent. We have checked for several cases that the energies are the same with an high accuracy as when geometry with the "usual" reflection plane is utilized. In Ref. [25] a Mn–O–Co superexchange was postulated to explain the oxygen-induced Mn–Co AF coupling. Since O at higher coverage readily penetrates below metal surfaces, we consider also the arrangement Mn overlayer—full O layer—Co slab (Mn/O/Co(0 0 1)). The Co–O distance is now taken 2.1 Å for reasons analogous to those specified above. Study of massive rearrangements comprising several layers or inclusion of possible noncollinear magnetic moments orientation is beyond the scope or the model.

3. Results and discussion

With two exceptions to be mentioned, the results are very similar for both Perdew–Wang and Langreth–Mehl–Hu density functionals. Results of our calculations based on the Perdew–Wang functional are displayed in Tables 1–4. We report the magnetization on oxygen, surface Mn or MnCo layer, and subsurface Co layer. The moments of the deeper Co layers fall roughly into the range 1.6–1.8 μ_B/atom, but the exact values depend on the details of calculation (choice of glide or reflection plane, number of layers). We make comparison of total energies for structures that differ only by orientation of magnetic moments. For geometrically differing structures the ASA approximation will introduce different errors since we study rather nonhomogeneous situations (considerable difference between metallic and oxygen atomic radii).

Table 3
Results for Mn/O/Co(0 0 1) systems (oxygen in the subsurface layer)

System	Mn1	Mn2	O	Co1(S-2)	Co2(S-2)	*E*
Mn (1×1)/O, F	3.46	3.46	−0.22	1.80	1.80	61
Mn (1×1)/O, AF	−3.30	−3.30	0.08	1.76	1.76	51
Mn $c(2\times2)$/O	3.55	−3.40	0.15	1.90	1.73	00

The meaning of symbols is the same as in Table 2. The subsurface Co layer, denoted now as S-2, contains two nonequivalent Co atoms. Atoms Mn*i* lie vertically above atoms Co*i* ($i = 1, 2$).

Table 4
Results for Mn/Co(0 0 1) systems with a $c(2\times2)$ oxygen overlayer ($\theta = 0.5$)

System	Exp	O	Mn	Co1(S-2)	Co2(S-1)	E
O $c(2\times2)$/Mn, F	0	−0.15	2.05	1.56	1.34	03
O $c(2\times2)$/Mn, AF	0	−0.01	−1.72	1.32	1.25	00
O $c(2\times2)$/Mn, F	10	−0.14	2.39	1.70	1.51	00
O $c(2\times2)$/Mn, AF	10	0.00	−2.12	1.47	1.34	13

The meaning of symbols is the same as in Table 1. All Mn atoms are equivalent, but there are two kinds of nonequivalent Co atoms in the subsurface layer. Exp (%) denotes the interlayer distance expansion between the Mn overlayer and subsurface Co layer, respectively.

The experiment finds [5,7] transition from a (2×2) structure with a ferromagnetic orientation of the Mn magnetic moment with the Co atoms to a (1×1) geometry with an antiferromagnetic coupling driven by oxygen. Our calculations indicate some destabilization of the F solutions by oxygen: For the $c(2\times2)$ alloy (Table 1) the F and AF solutions are practically degenerate in energy (with the Langreth–Mehl–Hu functional, the F solution is still more stable by 16 mRy than the AF one). For the (1×1) structures (Tables 2 and 3) the AF solutions are generally more stable than F ones. Nevertheless, with both exchange-correlation functionals, the AF solution with oxygen overlayer becomes unstable (Table 2) when the Mn–Co interlayer separation is expanded. For the Langreth–Mehl–Hu functional, on the other hand, the F solution with oxygen overlayer gets unstable for the nonrelaxed fcc geometry, and goes over into AF solution. In any case, the Mn antiferromagnetic (2×2) order remains energetically preferable structure (Table 2) for the Mn overlayer as it is in the absence of oxygen [13]. The same is true when the subsurface oxygen is considered (Table 3).

Our results show that oxygen has, as a rule, only moderate effect on the moment of Co. This is in agreement with experimental observation [7] but it is of little help in the geometry prediction. As mentioned in Ref. [5], the experimental estimation of the Mn moment is not quite reliable, but for the oxygen-free surface it seems to fall well below the theoretical value [8,13, Table 1]. Nevertheless, our Table 1 shows that for the surface MnCo alloy the moment of Mn is markedly suppressed by oxygen and the presence of residual oxygen [5] might reconcile the experimental and theoretical predictions. For well-oxidized surface, the experimental Mn moment is over 1 μ_B with antiparallel orientation with respect to Co atoms [5,7]. We find much smaller Mn moment for the oxidized Mn (1×1) AF overlayer and essentially

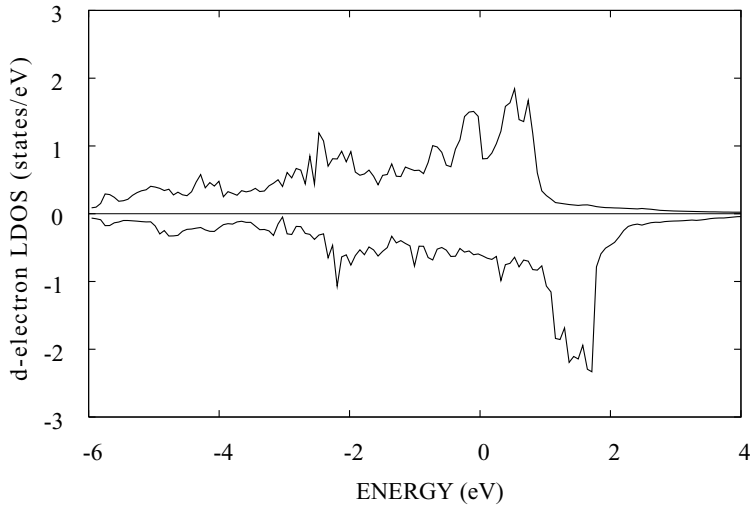

Fig. 1. Spin-resolved d-electron local density of states (LDOS) at the Mn atom for the O(1 × 1)/Mn/Co(0 0 1) system with ferromagnetic coupling between Mn and Co atoms, respectively. Positive (negative) LDOS values correspond to Mn states with spins parallel (antiparallel) to Co majority spins. The Fermi level coincides with the energy zero.

higher moments for remaining AF structures. Lets us note, however, that the magnetization seems to evolve continuously between the nonoxidized (2×2) structure and oxidized (1 × 1) overlayer [5,7]. This means that, at some stage at least, the surface has no well-defined structure (it can be, e.g. disordered). Besides that, at some intermediate oxygen coverage the experimentally established Mn moment is essentially zero. The experimentally observed small Mn moments might agree with our calculations supposing that experimentally intermediate oxygen doses correspond to our AF (1×1) solution (full oxygen coverage). However, when accepting such an ad hoc hypothesis, a question remains whether it is the energetically most favoured structure. We note also that oxygen is known to form often various forms of (sub)oxides at metal surfaces that do not allow an exact analysis. According to available theoretical studies [26] a massive oxide formation at metallic surfaces is expected to start at rather high oxygen coverage. If we suppose that the oxidized surface film is a Mn-rich disordered MnCo alloy film, the energetically favoured Mn $c(2 \times 2)$ can be hindered by the Co presence and the Mn moment can fall between the values we obtain for the oxidized forms of Mn (1 × 1) AF and MnCo $c(2 \times 2)$, respectively. Naturally, the surface can consist also of domains with different spin orientation that can explain the small (average?) Mn moment measured at intermediate oxygen doses. An invaluable information on the electronic structure below the Fermi level in magnetic crystals is provided by spin-resolved photoemission [27] or by similar techniques [28]. In Figs. 1–3 we display calculated spin-resolved densities of electronic states at the Mn overlayer for several differing magnetic arrangements. From these figures and from the data in Table 2, natural

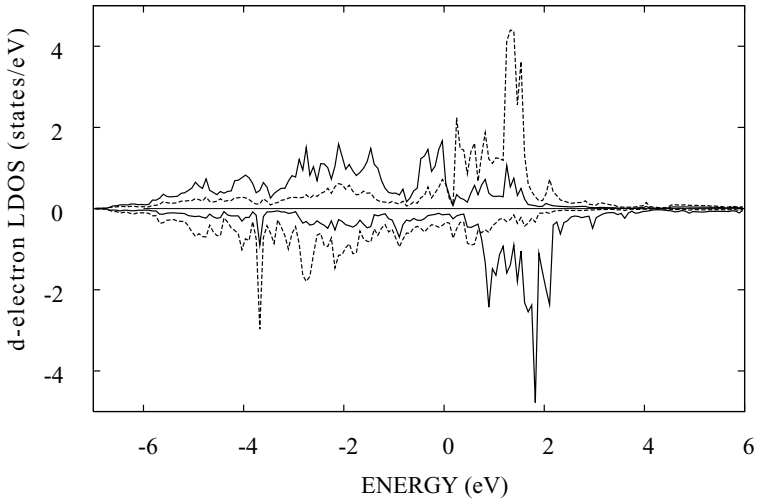

Fig. 2. The same as in Fig. 1 for the $c(2 \times 2)$ antiferromagnetic structure in the Mn layer. Full (dashed) lines correspond to the atom Mn1 (Mn2) in Table 2 that couples ferromagnetically (antiferromagnetically) to Co.

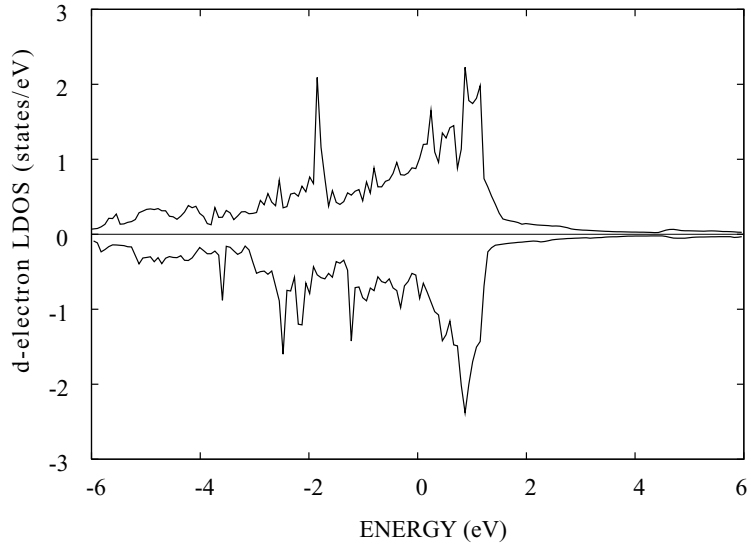

Fig. 3. The same as in Fig. 1 for antiferromagnetic coupling between Mn and Co atoms.

conclusions follow: (1) The spin up–spin down asymmetry is marked for overlayer with large magnetic moment because of large exchange splitting (Fig. 1). (2) For the same reason, in situations when the average Mn moment is low, the effective Mn d-band is wider supposing that magnetic moments on particular Mn atoms are high (Fig. 2) than if they are low (Fig. 3).

There is quite moderate magnetic moment induced on oxygen atoms. It couples in a number of cases (Tables 1–4) *antiferromagnetically* to its metallic neighbours, contrary to the situation typical for oxygen at Fe [29] and Co [22] surfaces. We have discussed the sign of the induced adsorbate magnetic moment in Refs. [22,30]. The difference might lie in the fact that the majority-spin bands are not so well filled in MnCo alloys [9] as in ferromagnetic Fe and Co. We refer the reader to Ref. [31] for possible consequences on the induced adatom orbital moment.

It is instructive also the possibility of noncomplete oxygen coverage. Some results are displayed in the Table 4 for an ordered $c(2 \times 2)$ oxygen overlayer corresponding to the coverage of $\theta = 0.5$. It is immediately seen that, contrary to the oxygen-free surface, the AF solution is more stable than the F one for the nonexpanded Mn overlayer. Hence, the destabilization of the F structure with respect to the AF arrangement (Table 2) takes place for noncomplete oxygen coverage (Table 4) as well.

Because of the lack of geometry optimization in our calculations, trends rather than decisive conclusions can be provided. The reason is that our values for Mn magnetic moments remain large in most cases (Tables 1–4) and, if no first-order transition is present, this fact cannot change due to a moderate geometry change. The Mn magnetic moments at oxygen coverage $\theta = 0.5$ lie between the values corresponding to $\theta = 0$ and 1, respectively. Hence, the Mn moments for the AF solution are quickly decreasing with oxygen coverage, at variance with the experimental data deduced for the high oxygen doses [5].

To conclude, our calculations show clear tendency to antiferromagnetic coupling between Mn and Co in the presence of oxygen, and confirm that, contrary to Co, magnetic moment of Mn is sensitive to oxygen presence. Open question is interpretation of the structure and magnetism evolution with the growing oxygen contamination. Our calculations indicate that simple models are not in accord with observations both because of the problem of the ground state and the magnetization magnitude. To explain completely the experimental data, one should probably have recourse to a disordered oxidized surface model such as an Mn-rich MnCo surface alloy. Another problems to be solved is the accuracy of Mn moment measurement and elucidation of its dependence on the oxygen coverage rather than on exposure. Our data give no support to antiferromagnetism based on a simple Mn–O–Co superexchange model.

Acknowledgements

The study has been facilitated by the Research Training Network “Computational Magnetoelectronics” HPRN-CT-2000-00143 of the European Commission.

References

[1] W.L. O’Brien, B.P. Tonner, Phys. Rev. B 50 (1994) 2963.
[2] A. Noguera, S. Bouarab, A. Mokrani, C. Demangeat, H. Dreyssé, J. Magn. Magn. Mater. 156 (1996) 21.
[3] O. Elmouhssine, Ph.D. Thesis, Strasbourg, 1998, unpublished results.
[4] S. Meza-Aguilar, Ph.D. Thesis, Strasbourg, 2001, unpublished results.
[5] W.L. O’Brien, B.P. Tonner, Phys. Rev. B 58 (1998) 3191.
[6] B.-Ch. Choi, J.P. Bode, J.A.C. Bland, Phys. Rev. B 58 (1998) 5166.

[7] Y. Yonamoto, T. Yokoyama, K. Amemiya, D. Matsumara, T. Ohta, Phys. Rev. B 63 (2001) 214406.
[8] S. Meza-Aguilar, O. Elmouhssine, H. Dreyssé, C. Demangeat, Phys. Rev. B 63 (2001) 064421.
[9] D. Wu, G.L. Liu, C. Jing, Y.Z. Wu, D. Loison, G.S. Dong, X.F. Jin, D.-S. Wang, Phys. Rev. B 63 (2001) 214403.
[10] A. Sandell, P.H. Andersson, E. Holmström, A.J. Jaworowski, L. Nordström, Phys. Rev. B 65 (2001) 035410.
[11] S. Blügel, Appl. Phys. A: Mater. Sci. Process. 63 (1996) 595.
[12] D. Hobbs, J. Hafner, J. Phys.: Condens. Mat. 13 (2001) L681.
[13] B. M'Passi-Mabiala, S. Meza-Aguilar, C. Demangeat, Phys. Rev. B 65 (2002) 012414.
[14] D.C. Langreth, M.J. Mehl, Phys. Rev. B 28 (1983) 1809.
[15] C.D. Hu, D.C. Langreth, Phys. Scripta 32 (1985) 391.
[16] J.P. Perdew, Y. Wang, E. Engel, Phys. Rev. Lett. 66 (1991) 508.
[17] C. Demangeat, J.C. Parlebas, Rep. Prog. Phys. 65 (2002) 1679.
[18] G. Krier, M. van Schilfgaarde, A.T. Paxton, O. Jepsen, O.K. Andersen, TB-LMTO-ASA Programme, Version 47, Max-Planck-Institut für Feskörperforschung, Stuttgart, 1995 (revised, 1998).
[19] K.H. Hellwege (Ed.), Landolt-Börnstein Zahlenwerte und Funktionen, Band I/4, Springer, Berlin, 1955, pp. 86 and 131.
[20] M.P. Pascal, C.R. Acad. Sci. Paris C 264 (1967) 1270.
[21] G. Comelli, V.R. Dhanak, M. Kiskinova, K.C. Prince, Surf. Sci. Rep. 32 (1998) 167.
[22] Š. Pick, H. Dreyssé, Surf. Sci. 474 (2001) 64.
[23] M.V. Ganduglia-Pirovano, M. Scheffler, Phys. Rev. B 59 (1999) 15533.
[24] B. Lazarovits, L. Szunyogh, P. Weinberger, Phys. Rev. B 65 (2002) 104441.
[25] S. Andrieu, E. Foy, H. Fischer, M. Alnot, F. Chevrier, G. Krill, M. Piecuch, Phys. Rev. B 58 (1998) 8210.
[26] W.-X. Li, C. Stampfl, M. Scheffler, Phys. Rev. B 67 (2003) 045408, and references therein.
[27] M. Getzlaff, J. Bansmann, J. Braun, G. Schönhense, J. Magn. Magn. Mater. 161 (1996) 70.
[28] S. Förster, G. Baum, M. Müller, H. Steidl, Phys. Rev. B 66 (2002) 134427.
[29] Š. Pick, H. Dreyssé, Surf. Sci. 394 (1997) 192.
[30] Š. Pick, H. Dreyssé, Surf. Sci. 460 (2000) 153.
[31] K. Amemiya, T. Yokoyama, Y. Yonamoto, D. Matsumara, T. Ohta, Phys. Rev. B 64 (2001) 132405.